Average kinetic energy of atoms in a solid measured with resonant nuclear reactions

M. Berheide,* W. H. Schulte, H.-W. Becker, L. Borucki, M. Buschmann, N. Piel, and C. Rolfs
Institut für Experimentalphysik III, Ruhr-Universität Bochum, D-44780 Bochum, Germany

G. E. Mitchell
North Carolina State University, Raleigh, North Carolina 27695
and Triangle Universities Nuclear Laboratory, Durham, North Carolina 27708

J. S. Schweitzer
Department of Physics, University of Connecticut, Storrs, Connecticut 06269
(Received 20 May 1998)

Solid neon samples at 8 ± 2 K and under vapor pressure were used to measure yield curves of the 272-keV nuclear resonance in the $^{21}\mathrm{Ne}(p,\gamma)^{22}\mathrm{Na}$ reaction. The Doppler broadening of the narrow resonance due to target atom motion was determined with very good beam energy resolution. The average kinetic energy of single neon atoms in the solid due to their motion in the beam direction was $E_{kin,z}=1.06\pm0.2$ meV (corresponding to an average kinetic energy of $E_{kin}/k=37\pm7$ K). This value is in good agreement with published values obtained from neutron Compton scattering and from path-integral Monte Carlo calculations. [S0163-1829(98)07142-2]

The average kinetic energy of atoms in a solid sample is correlated with the mean square of the velocity distribution of the sample atoms. The mean-square velocity of atoms in a solid has been measured directly in only a few cases, although it is of considerable interest, especially for quantum solids. However, it is well known that the velocity distribution leads to Doppler broadening of resonances in absorption measurements. The Doppler effect on resonant reactions with neutrons was first considered by Bethe[1] and later refined by Lamb.[2] In this paper we present a measurement of the average kinetic energy of an atom in a solid sample with nuclear reaction analysis (NRA) involving a proton beam of very high energy resolution. The Doppler broadening of a nuclear resonance was determined separately from effects due to projectile energy loss. We compare these results with data from neutron Compton scattering (NCS), with the value deduced from the Debye temperature, and with results from path-integral Monte Carlo (PIMC) calculations.[3–5]

In a nuclear reaction with charged particles, the recoil energy is much larger than the binding energy of the target atoms. For this reason, final-state effects involving the target atoms may be neglected.[2] If a Maxwell distribution of the single-atom velocities is assumed, the width (full width at half maximum) of the Doppler broadening ΔE_D is given to first order by

$$\Delta E_D = 4\left(2\ln 2\frac{m_p}{m_t}E_R E_{kin,z}\right)^{1/2}, \tag{1}$$

where E_R is the resonance energy, $E_{kin,z}$ is the average kinetic energy of the sample atom due to its motion in the beam direction, and m_t and m_p are the masses of the target atom and the projectile. However, for nuclear resonances initiated by charged particles, Doppler broadening is intertwined with effects due to the stopping of charged particles in matter, namely, the small energy losses of the projectiles to electrons in the target atoms.[6–9] The resonance curve may be considered a convolution of several contributions. One contribution is given by the cross section of the nuclear reaction around the resonance energy, which for an isolated resonance is assumed to be a Lorentzian of width Γ. Another contribution is a Gaussian of width ΔE_G, which is a combination of the energy spread of the ion beam ΔE_p and the Doppler broadening ΔE_D. The convolution of these symmetric contributions yields a Voigt curve with a width ΔE_V approximately given by

$$\Delta E_V = \frac{\Gamma}{2}+\left(\frac{\Gamma^2}{4}+\Delta E_D^2+\Delta E_p^2\right)^{1/2}. \tag{2}$$

The final contribution is called the energy-loss spectrum and is a complicated function of both the target parameters and the projectile type and energy. The energy-loss spectrum is asymmetric and primarily determines the behavior of the line shape in the region above the resonance energy. In the rare case that a threshold energy exists for projectile energy losses that is larger than the width ΔE_V, it is possible to extract the Doppler broadening without sensitivity to the choice of the energy-loss model. This leads to the unusual requirement that the Doppler broadening must be small in order to be measured precisely.

A few years ago, we demonstrated that one can extract Doppler broadening in resonant reactions with Ne gas, where the ionization energy is exceptional high.[8] These measurements utilized the $^{21}\mathrm{Ne}(p,\gamma)^{22}\mathrm{Na}$ reaction at 272-keV proton energy and a high-purity ^{21}Ne gas target cooled to a temperature of about 25 K to reduce the Doppler broadening. The measured Doppler broadening was consistent with the velocity distribution of atoms in an ideal gas [Eq. (1) with $E_{kin,z}=kT/2$, where k is the Boltzmann constant and T the temperature].[1]

In this paper measurements are described for the same resonance in a neon solid (^{21}Ne). Due to the low sublimation point of neon, the experiment had to be performed at a temperature below 10 K. In order to guarantee a pure neon target, an ultrahigh vacuum (UHV) setup was employed. Details of the experimental setup are given in earlier publications.[10,11] In short, the setup consists of a set of metal-sealed UHV chambers installed at the high-energy-resolution 400-kV ion accelerator at the University of Münster. The gas pressure ranges from 1×10^{-4} Pa in the beam line to below 1×10^{-8} Pa in the target chamber. The protons are provided by a hollow cathode ion source. The ions are extracted with an electrode at a potential of 7 kV that is provided by a high-stability power supply. The terminal voltage is generated by a Cockroft-Walton cascade and measured with a precision voltmeter at a resistance voltage divider. The remaining ac ripple of the terminal voltage is measured with a pickup plate mounted above the accelerator. The measured ac signal is amplified by a calibrated factor and then applied to the electrically insulated target (ripple compensation technique).[8] With this method an energy resolution of about 10 eV is obtained at a beam energy of $E_p=272$ keV ($\Delta E_p/E_p=4\times10^{-5}$).

The beam is defined by two apertures and a deflection unit and can be swept over a 10 mm$\times$10 mm area in order to reduce the current density at the target surface. The beam current is measured with a precise rotating wire dosimeter. The target zone consists of a gold-covered copper end of an helium evaporation cryostat shielded by a copper cylinder that is connected to the first cooling stage of the helium evaporation cryostat. A 25 mm$\times$10 mm hole in the cylinder serves as a beam entrance and a viewport. A 3-mm copper tube connected to a gas purifier serves as an entrance for the neon gas. The temperature of the target is monitored by a four-point measurement on a platinum resistor mounted at the cryostat head. A 7.6 cm$\times$7.6 cm NaI(Tl) detector is located 5 cm from the beam spot. The detector signals are processed with standard nuclear electronics to count the detected γ rays between 3 and 7 MeV. A personal computer automatically varies the high voltage at the terminal over a predefined interval and records terminal voltage, count rate, beam current, time, temperature, and pressure in the target chamber.

Prior to the measurement on the solid, the energy spread of the ion beam at the resonance energy of 272 keV was determined by measuring the yield curve of the resonance with a neon gas target at 12 ± 2 K. Since the Doppler broadening can be calculated precisely for monoatomic gas targets (see above), the energy spread of the ion beam could be determined: $\Delta E_p=10.6\pm1.5$ eV.[11] Immediately afterwards, the solid target setup described above was installed. When a pressure in the target chamber below 1×10^{-8} Pa was obtained, neon gas (isotopically enriched to 94% in ^{21}Ne), was brought into the copper cylinder and the cryostat was cooled with a liquid-helium flow of 25 l/h. Under these conditions, a neon solid started to grow on the substrate of the cryostat.

After several minutes a proton beam of about 1.5 μA was focused on the target area with the beam axis perpendicular to the target surface. During the measurement the beam was swept over an area of 7 mm$\times$7 mm. Under these conditions a stable temperature of 8 ± 2 K was obtained at the cryostat head. The continuous neon gas flow was adjusted such that the sputtering loss of neon at the solid surface was compensated by the growth rate of the solid in the neon atmosphere. The increased pressure in the target chamber of about 8×10^{-5} Pa (ion gauge reading corrected to Ne gas) was still sufficiently low to prevent significant projectile energy losses on gas atoms. The quality of the solid was monitored during the experiments by the color and the intensity of the stimulated luminescence. The beam spot was of an almost homogeneously light-violet-colored rectangular shape. Figure 1 shows the part of the yield curve around the resonance energy E_R taken with this target. The data points are sums over six independent sweeps in energy steps of about 1 eV over the range from 100 eV below the resonance to 400 eV above the resonance. Since each individual sweep has the same line shape, energy shifts, and target changes during the measurement period can be neglected. The plateau at higher energies represents the thick-target yield of a nuclear reaction that can be described by assuming an averaged stopping power for charged particles of the target material. Note the intense peak at the resonance energy that is given by those nuclear reactions that are not affected by energy losses of the projectiles. The gap between peak and plateau is caused by the discrete nature of the energy loss, which in turn is an effect of the binding energy of the electrons in the solid.

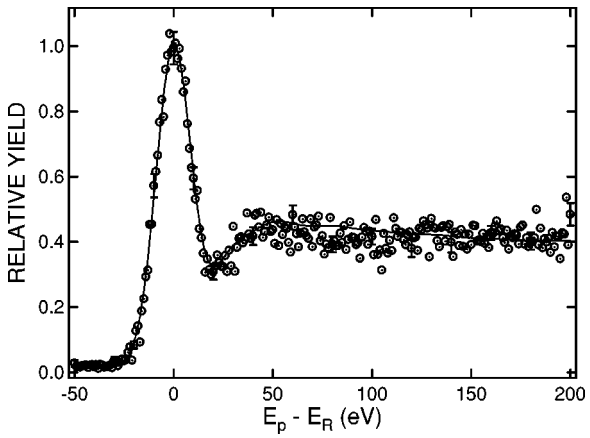

FIG. 1. Thick-target yield curve of the 272-keV resonance in ^{21}Ne$(p,\gamma)^{22}$Na on solid neon. Some data points are shown with typical error bars. The solid line represents a fit (see text for details). The yield is normalized to the maximum value of the fit. Energies are given relative to the resonance energy.

In a first-order treatment of the yield curve a Voigt function was fit to the rising edge. The result was a width $\Delta E_V=21.6$ eV. A more thorough analysis was performed by correcting for the influence of those nuclear reactions in which the projectiles undergo an energy loss with target electrons. The solid line in Fig. 1 represents a best fit using a convolution of a Voigt curve with a sophisticated energy-loss spectrum. Details of the evaluation of an energy-loss spectrum are given by Schulte *et al.*[9] In short, a Monte Carlo simulation is performed in which the energy-loss spectrum is generated by monitoring the energy losses of a large number of projectiles. The energy loss of a single projectile is considered as a sum of discrete energy losses caused by single collisions with electrons in the neon atoms.[6] The number of collisions follows a Poisson distribution and the most prob-

able number of collisions for a single projectile is a function of the target thickness and the cross section for a single collision. The problem is thus reduced to determining the energy-loss spectrum for a very thin target in which not more than one collision occurs.

Here we assume that the probability of an energy loss with a certain energy transfer in a single encounter decreases approximately with the square of the transferred energy (the Thomson model). In a collision with a target atom, a lower limit for the energy loss of a projectile is the electron binding energy plus the minimum recoil energy, which is transferred to the neon atom due to the binding of the electron to the nucleus. The fact that a neon atom contains electrons with different binding energies E_i was taken into account by adding two probability functions: one for the electrons of the $L1$ shell ($E_i=48$ eV) and the other for the $L2$ and $L3$ shells ($E_i=22$ eV). The K shell contributes only to large energy transfers and was neglected here. Since the number of electrons in the $L2/L3$ shells is three times the number in the $L1$ shell, the corresponding probabilities were multiplied by 3. This somewhat arbitrary estimate gives better agreement with experimental data than more detailed atomic physics models, which seem to underestimate the influence of the $L2/L3$ shells.[9,12] The total probability for an energy loss was adjusted such that the energy-loss spectra agreed with measurements on neon-gas targets and with the stopping power.

The energy-loss spectrum obtained with this method was fitted by convoluting with Voigt curves of different Lorentzian and Gaussian contributions. The best fit to the data is a Voigt curve with a total width $\Delta E_V=20.9\pm1.0$ eV. (This is only 0.7 eV less than a fit to the rising edge alone, thus demonstrating the excellent separation between broadening and energy-loss effects.) With a resonance width $\Gamma=1.0^{+1.0}_{-0.7}$ eV, given by the Lorenzian contribution of fits to all available yield curves, and an energy spread of the ion beam $\Delta E_p=10.6\pm1.5$ eV (see above), we determined a Doppler broadening $\Delta E_D=17.4\pm1.6$ eV [Eq. (2)]. From Eq. (1) one obtains an average kinetic energy of the atom due to its motion in the beam direction of $E_{kin,z}=1.06\pm0.20$ meV. With the assumption of isotropic motion of the single atom, we get the average kinetic energy per atom $E_{kin}=3.18\pm0.60$ meV or $E_{kin}/k=37\pm7$ K.

The average kinetic energy of an atom in a solid sample can be calculated in the Debye model:

$$E_{kin}=\frac{9}{2}kT\left(\frac{T}{\theta_D}\right)^3\int_0^{\theta_D/T}t^3\left(\frac{1}{e^t-1}+\frac{1}{2}\right)dt. \qquad (3)$$

The low-temperature limit ($T\ll\theta_D$) of Eq. (3) is $E_{kin}=9k\theta_D/16$. The Debye temperature of the ^{21}Ne solid at $T=8\pm2$ K was interpolated from Ref. 13 to be $\theta_D=66\pm4$ K, yielding $E_{kin}/k=37\pm2$ K in very good agreement with the experimental value.

Figure 2 and Table I show the average kinetic energies determined in this experiment and by other experimental methods, as well as calculated values taken from the literature. The long-dashed line gives the expected values for a ^{21}Ne-gas target. The solid line gives the values predicted from Eq. (3) with a Debye temperature $\theta_D=66$ K. A direct measurement of mean-square velocities is given by neutron-Compton-scattering measurements on solid neon of natural isotopic concentration.[3,4] NCS measures the average momentum distribution of sample atoms by determining the broadening of a time-of-flight distribution of incoherently scattered energetic neutrons. The calculated values are based on a path-integral Monte Carlo approach, where the motion of a small set of sample atoms is followed in detail using anharmonic interatomic potentials. Thermodynamic properties are derived by averaging over time. Note that the errors of these calculations as listed in Table I do not include changes with the choice of the interatomic potential and other systematic errors. [Incidentally, the results of the PIMC calculations can

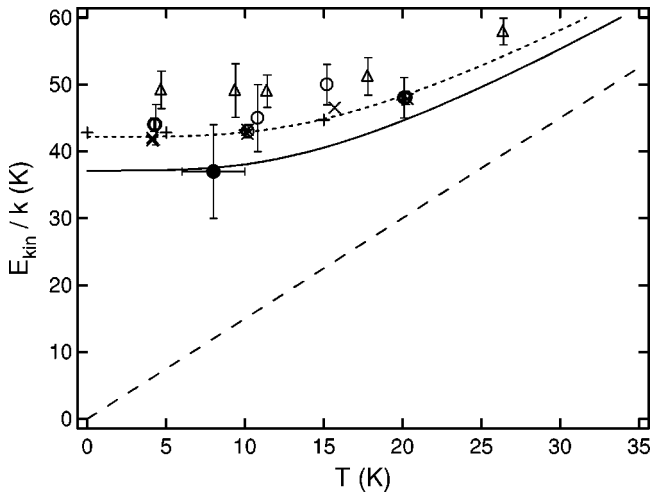

FIG. 2. Average kinetic energy of single neon atoms vs sample temperature. The experimental value obtained in this work (●) is compared with values from neutron Compton scattering [△ (Ref. 3), ○ (Ref. 4)] and path-integral Monte Carlo calculations [× (Ref. 4), + (Ref. 5)]. The curves represent an ideal gas (long-dashed line) and solids in the Debye model with $\theta_D=66$ K (solid line) and $\theta_D=75$ K (short-dashed line).

TABLE I. Measured and calculated single particle kinetic energy of solid neon below 10 K.

Method	Ref.	T (K)	E_{kin}/k (K)
NRA [a]	This work	8 ± 2	37 ± 7 [b]
NCS [c]	3	4.7 ± 0.1	49.2 ± 2.8
		9.4 ± 0.1	49.1 ± 4.0
NCS [c]	4	4.25 ± 0.05	44 ± 1
		10.2 ± 0.1	43 ± 1
Debye model	This work [d]	8 ± 2	37 ± 2
PIMC, [e] LJ [f]	5	5 ± 0	42.8 ± 0.1
		10 ± 0	43.2 ± 0.1
PIMC, [e] HFD-C [g]	4	4.125 ± 0	41.6 ± 0.1
		10.154 ± 0	42.6 ± 0.1
PIMC, [e] LJ [f]	4	4.125 ± 0	42.0 ± 0.3
		10.154 ± 0	43.2 ± 0.1

[a]Nuclear reaction analysis.
[b]For ^{21}Ne solid, including surface effect, see text.
[c]Neutron Compton scattering.
[d]Equation (3) with $\Theta_D=66\pm4$ K.
[e]Path-integral Monte Carlo calculations.
[f]Lennard-Jones potential.
[g]Aziz HFD-C potential.

be approximated by using Eq. (3) with $\theta_D = 75$ K as shown by the short-dashed line in Fig. 2.] Our value for the kinetic energy of neon is in good agreement with the more recent NCS data and PIMC calculations of Refs. 4 and 5 and within two standard deviations of the NCS values of Ref. 3.

Note that for two reasons the average single-particle kinetic energy determined in this work is not expected to be exactly the same as for the NCS measurements and the calculations. The first reason is that our measurement was performed with ^{21}Ne that has a single-particle kinetic energy about 1 K smaller than natural neon [with $\Theta_D = 68$ K at $T = 8$ K (Ref. 13)]. The second reason is that the resonance peak in the yield curve is sensitive to atoms near the solid surface, while neutron scattering is more sensitive to bulk atoms. Elsewhere[11] it was discussed that the weaker binding of surface atoms compared with bulk atoms in a solid reduces Doppler broadening. An estimation of the surface effect on our measurement using slab model calculations by Allen and de Wette[14] yields a single-particle kinetic energy 2 K lower. Thus we expect that E_{kin} at $T = 8$ K measured with the (p,γ) reaction should be about 3 K lower than the neutron-Compton-scattering value. However, the fact that our value of E_{kin}/k is more than 3 K below the measurement and calculations from Refs. 3–5 should not be interpreted as strong evidence for a special model of solid surface dynamics because the experimental uncertainties are still too large.

These measurements demonstrate that nuclear reactions with charged particles can be used to measure the dynamics of atoms in solids. It may even be possible to extract information about surface dynamics. An advantage of this method is that the momentum of the charged particle in a nuclear reaction is much larger than the momentum of the sample atom, meaning that final-state atomic effects may be neglected. This is not always the case for neutron Compton scattering. Having established the approximate equivalence of the two methods, one could now adopt the single-particle values from the neutron measurements, use the resulting value for the Doppler spread in the analysis of poorer resolution resonance data, and determine the experimental energy-loss spectra. This would be of considerable interest for testing energy-loss models of charged particles in matter.

We would like to thank Professor R. Santo and H. Baumeister for their support of the experiments. This work was supported in part by Deutsche Forschungsgemeinschaft (Ro429/16-3), U.S. Department of Energy (Grant No. DE-FG02-97-ER41042), Minister für Wissenschaft und Forschung des Landes NRW (IVA5-10600387), and Schlumberger-Doll Research.

*Present address: Schlumberger-Doll Research, Ridgefield, CT.

[1] H. A. Bethe, Rev. Mod. Phys. **9**, 140 (1937).
[2] W. E. Lamb, Phys. Rev. **55**, 190 (1939).
[3] D. A. Peek, I. Fujita, M. C. Schmidt, and R. O. Simmons, Phys. Rev. B **45**, 9680 (1992).
[4] D. N. Timms, A. C. Evans, M. Boninsegni, D. M. Ceperley, J. Mayers, and R. O. Simmons, J. Phys.: Condens. Matter **8**, 6665 (1996).
[5] A. Cuccoli, A. Macchi, V. Tognetti, and R. Vaia, Phys. Rev. B **47**, 14 923 (1993).
[6] H. W. Lewis, Phys. Rev. **125**, 937 (1962).
[7] J. M. Donhowe, J. A. Ferry, W. G. Mourad, and R. G. Herb, Nucl. Phys. A **102**, 383 (1967).
[8] W. H. Schulte, H. Ebbing, S. Wüstenbecker, H.-W. Becker, M. Berheide, M. Buschmann, C. Rolfs, G. E. Mitchell, and J. S. Schweitzer, Nucl. Instrum. Methods Phys. Res. B **71**, 291 (1992).
[9] W. H. Schulte, H. Ebbing, H.-W. Becker, M. Berheide, M. Buschmann, C. Rolfs, G. E. Mitchell, and J. S. Schweitzer, J. Phys. B **27**, 5271 (1994).
[10] M. Berheide, H.-W. Becker, M. Buschmann, N. Piel, C. Rolfs, W. H. Schulte, G. E. Mitchell, and J. S. Schweitzer, Nucl. Instrum. Methods Phys. Res. B **99**, 289 (1995).
[11] M. Berheide, H.-W. Becker, L. Borucki, M. Buschmann, N. Piel, C. Rolfs, W. H. Schulte, G. E. Mitchell, and J. S. Schweitzer, Nucl. Instrum. Methods Phys. Res. B **118**, 483 (1996).
[12] P. Kürpick, J. Phys. B **29**, L169 (1996).
[13] E. Somoza and H. Fenichel, Phys. Rev. B **3**, 3434 (1971).
[14] R. E. Allen and F. W. de Wette, Phys. Rev. **179**, 873 (1969).